Eicosapentaenoic acid plays a role in stabilizing dynamic membrane structure in the deep-sea piezophile *Shewanella violacea*: a study employing high-pressure time-resolved fluorescence anisotropy measurement

Keiko Usui[1], Toshiki Hiraki[1], Jun Kawamoto[2], Tatsuo Kurihara[2], Yuichi Nogi[1], Chiaki Kato[1], and *Fumiyoshi Abe[1,2,3]

[1]Institute of Biogeosciences, Japan Agency for Marine-Earth Science and Technology (JAMSTEC); [2]Institute for Chemical Research, Kyoto University; [3]Department of Chemistry and Biological Science, College of Science and Engineering, Aoyama Gakuin University

*Corresponding author: Fumiyoshi Abe

Department of Chemistry and Biological Science, College of Science and Engineering, Aoyama Gakuin University

5-10-1 Fuchinobe, Chuo-ku, Sagamihara 252-5258, Japan

Phone: +81-42-759-6233

Fax: +81-42-759-6511

E-mail: abef@chem.aoyama.ac.jp

Keywords: *Shewanella violacea*; high hydrostatic pressure; EPA; TMA-DPH; time-resolved fluorescence anisotropy measurement; membrane fluidity

Abbreviations: EPA, eicosapentaenoic acid; POPC, palmitoyl-oleylphosphatidylcholine; UFA, unsaturated fatty acid; MUFA, monounsaturated fatty acid; PUFA, polyunsaturated fatty acid; DPH, 1,6-diphenyl-1,3,5-hexatriene; TMA-DPH, 1-[4-(trimethylamino)pheny]-6-phenyl-1,3,5-hexatriene; TCSPC, time-correlated single-photon counting; r_s, steady-state anisotropy; r_0, maximum anisotropy; r_∞, limiting anisotropy; θ, rotational correlation time; S, order parameter; D_w, rotational diffusion coefficient; τ, fluorescence lifetime; HP-TRFAM, high-pressure time-resolved fluorescence anisotropy measurement

Abstract

Shewanella violacea DSS12 is a psychrophilic piezophile that optimally grows at 30 MPa. It contains a substantial amount of eicosapentaenoic acid (EPA) in the membrane. Despite evidence linking increased fatty acid unsaturation and bacterial growth under high pressure, little is known of how the physicochemical properties of the membrane are modulated by unsaturated fatty acids *in vivo*. By means of the newly developed system performing time-resolved fluorescence anisotropy measurement under high pressure (HP-TRFAM), we demonstrate that the membrane of *S. violacea* is highly ordered at 0.1 MPa and 10 °C with the order parameter S of 0.9, and the rotational diffusion coefficient D_w of 5.4 μs^{-1} for 1-[4-(trimethylamino)pheny]-6-phenyl-1,3,5-hexatriene in the membrane. Deletion of *pfaA* encoding the omega-3 polyunsaturated fatty acid synthase caused disorder of the membrane and enhanced the rotational motion of acyl chains, in concert with a 2-fold increase in the palmitoleic acid level. While the wild-type membrane was unperturbed over a wide range of pressures with respect to relatively small effects of pressure on S and D_w, the Δ*pfaA* membrane was disturbed judging from the degree of increased S and decreased D_w. These results suggest that EPA prevents the membrane from becoming hyperfluid and maintains membrane stability against significant changes in pressure. Our results counter the generally accepted concept that greater fluidity is a membrane characteristic of microorganisms that inhabit cold, high-pressure environments. We suggest that retaining a certain level of membrane physical properties under high pressure is more important than conferring membrane fluidity alone.

1. Introduction

High hydrostatic pressure and low temperature characterize the majority of oceanic environments in terms of the volume occupied. Deep-sea organisms have adapted to survive under such extreme conditions [1–3]. High pressure and low temperature exert profound physiological impacts on biological membranes, primarily resulting in tighter packing and restricting the rotational motion of acyl chains [4, 5]. It is assumed that the functions of membrane proteins such as electric transport, nutrient uptake, ion influx, and receptor activation are diminished by high pressure because these functions largely depend on an appropriate membrane structure [4, 6–8]. Therefore, the maintenance of appropriate membrane fluidity is crucial for life under low-temperature and high-pressure conditions. The packing effects of membranes are circumvented by modifying the lipid compositions in a broad range of organisms. Generally, cold adaptation is associated with the incorporation of greater proportions of unsaturated fatty acids (UFAs) [9–11]. Fatty acids containing one or more double bonds take a more expanded conformation than their counterparts with saturated bonds. The large free volume created within intermolecular spaces allows greater conformational freedom of acyl chains and less packing of the lipids. Consequently, the membrane becomes more fluid. This homeostatic adaptation has been termed “homeoviscous adaptation” [7, 12]

Elevated hydrostatic pressure orders lipid membranes in a manner analogous to lowering temperature. For example, a pressure increase by 100 MPa increases the main transition

(L_β/L_α) temperature of the stearoyloleylphosphatidylcholine (SOPC) and dioleylphosphatidylcholine (DOPC) membrane by 18.1 °C and 23.3 °C, respectively [13]. Macdonald and colleagues investigated the fluidity of the membranes of a number of fish that were confined to the shallow-water zone or the deep ocean floor by means of fluorescence anisotropy measurement. Anisotropy of 1,6-diphenyl-1,3,5-hexatriene (DPH) in the brain myelin was compared between different species of the genus *Coryphenoides* which lived over different depth ranges and was distinctly lower in deep-sea species, indicating a lower order of the membrane [14]. The fatty acid composition of phosphatidylcholine and phosphatidylethanolamine in liver mitochondria was also compared among different species [15]. The ratio of UFAs to saturated fatty acids showed a statistically significant increase with depth of capture, implying the acclimation of fish membranes to ambient pressure. Similarly, many high-pressure-adapted bacteria (termed piezophiles) in the deep sea contain high proportions of UFAs in their membrane lipids, which in some cases increase with increasing growth pressure [16-19]. Particularly, the occurrence of omega-3 polyunsaturated fatty acids (PUFAs) such as eicosapentaenoic acid (EPA; C20:5) and docosahexaenoic acid (DHA; C22:6) within phospholipids is a characteristic of piezophiles and psychrophiles that are adapted to cold environments [20, 21]. Because of their extremely low melting temperatures, the incorporation of PUFAs is thought to exert a significant promoting effect on membrane fluidity. While the main transition temperature of the distearoylphosphatidylcholine (DSPC) membrane is 55.6 °C, that of stearoyl-oleylphosphatidylcholine (SOPC) and stearoyl-arachidonoylphosphatidylcholine (SAPC) is 6.7 °C and –13.0 °C, respectively [22]. However, the criterion of incorporating double bonds in membrane fatty acids is not always

relevant to biological significance in homeoviscous adaptation [12]. According to the thermodynamic properties of phase transitions in artificial lipid bilayers, the volume change (ΔV) associated with the gel-to-liquid crystalline phase is 31.6 ml/mol, 18.9 ml/mol, and 10.1 ml/mol in the DSPC, SOPC, and SAPC membrane, respectively [22]. The clear difference in the ΔV can be explained on the basis of the large free volumes of UFAs in the gel phase without any significant difference in their volumes in the liquid crystalline phase. In the stearoyl-docosahexanoylphosphatidylcholine (SDPC) membrane, the polyunsaturated fatty acyl chains take a helical configuration, which reduces the effective chain length and stabilizes the gel phase [23]. Because biological membranes are complex mixtures of lipids in terms of the chain length, degree of unsaturation, polar head species, and proportion of individual phospholipids in a membrane, the role of monounsaturated fatty acids (MUFAs) and PUFAs on membrane properties cannot be understood straightforwardly. EPA and DHA also have clinical importance in human health and development. These PUFAs serve as precursors for hormones such as inflammatory mediators [24]. DHA, which is synthesized from EPA as a precursor, constitutes the major PUFA of brain lipids [25]. It has beneficial effects on cognition and learning ability and inhibits amyloid levels in the cerebral cortex of Alzheimer's disease model rats [26]. Nevertheless, the effects of PUFAs on the structural properties of the plasma membrane of nerve cells is still unclear.

The distribution of EPA-producing bacteria in the environment has been considered as evidence of a requirement for EPA for growth under cold, high-pressure conditions. Particularly, numerous deep-sea bacteria contain substantial amounts of PUFAs, leading to the speculation that PUFAs have a role in membrane-mediated functions [17, 27-29]. The

deep-sea piezophile *Photobacterium profundum* strain SS9 contains EPA at a proportion of 11 % when cultured under the optimal growth conditions (28 MPa, 9 °C). It was reported that a mutant lacking EPA production exhibits normal growth under high pressure and low temperature, whereas another mutant defective in the production of oleic acid fails to grow under the same conditions [17]. Accordingly, MUFAs but not PUFAs are required for growth in this bacterium under high pressure and low temperature. In the cold-adapted bacterium *Shewanella livingstonensis* Ac10 isolated from Antarctic seawater, EPA plays a role in organizing the cytoplasmic membrane at low temperature [30]. However, it may not be required for the maintenance of membrane fluidity, based on the finding that the diffusion rate of a small lipophilic molecule, pyrene, in the membrane was almost identical between the wild-type strain and the EPA-deficient mutant. Instead, EPA is specifically required for normal cell division at low temperature [30]. *Shewanella piezotolerans* WP3 isolated from a sediment sample of the western Pacific Ocean at the depth of 1,914 m is a psychrotolerant and piezotolerant bacterium, growing optimally at 15–20 °C under pressures of 0.1–20 MPa [31]. *S. piezotolerans* cells contain EPA in the membrane. The loss of EPA results in growth defects at low temperature (4 °C, 0.1 MPa) and high pressure (20 °C, 20 MPa), indicating the requirement of EPA under the extreme conditions [19]. *Shewanella violacea* strain DSS12 is a deep-sea bacterium isolated from the Ryukyu Trench at the depth of 5,110 m. It exhibits moderate piezophily with optimal growth at 30 MPa and 8 °C but it can also grow at 0.1 MPa [32]. The exploration of the piezophily of this bacterium has become an active area of research in deep-sea microbiology with respect to taxonomy, gene expression, protein function, and the respiratory system [32–35]. Its complete genome sequence is available to

the public [36]. *S. violacea* cells contain a substantial amount of EPA in the membrane. EPA also plays a role in cell division under high pressure because an EPA-deficient *S. violacea* mutant displayed filamentation at 30 MPa [37]. Although the functional and physiological significance of microbial EPA is evident, its role in dynamic membrane structure under low temperature and high pressure remains to be resolved.

Fatty acid analysis provides valuable information on membrane physiology, although the variability in lipid composition and complexity of lipid behavior that occur in a heterogeneous natural cell membrane make it difficult to characterize how the physicochemical properties of the membrane respond to varied environmental conditions. To achieve an understanding of the role of UFAs, it is necessary to quantify membrane fluidity *in vivo* in terms of membrane order, rotational motion of acyl chains, or lateral diffusion of lipid molecules. Of the spectroscopic techniques available to study membrane properties, fluorescence anisotropy measurement is a common useful method providing information on dynamic membrane properties [38–40]. Although this technique has been widely employed for the study of model membranes, few results have been reported in whole, living cell systems. DPH and its cationic derivative 1-[4-(trimethylamino)pheny]-6-phenyl-1,3,5-hexatriene (TMA-DPH) are commonly used for such analyses. DPH primarily distributes perpendicular to the bilayer plane near the center of the membrane but partially distributes parallel to it within the acyl chain tails [39]. TMA-DPH is anchored at the lipid–water interface due to its charged moiety and thereby reflects only the interfacial region of the membrane. Trevors and colleagues have been extensively investigating structural and chemical changes that occur in bacterial membranes exposed to varied environmental factors including temperature, ions, pH, and

chemicals [41, 42].

In this study, we developed a new system to enable fluorescence anisotropy measurement under high pressure. Using this system, we elucidated the dynamic properties of the membrane in *S. violacea* cells under high pressure to elucidate the structural role of EPA in this bacterium. Specifically, we employed time-resolved fluorescence anisotropy measurement based on time-correlated single-photon counting (TCSPC), which provided quantitative information on membrane order, rotational motion of acyl chains, and the degree of water penetration within the membrane in a single measurement. Our results revealed an unexpected action of EPA to maintain cell membrane rigidity and to affect membrane hydration under varied pressure conditions.

2. Materials and methods

2.1. Bacterial strain and culture conditions

A laboratory stock of *S. violacea* strain DSS12 (wild type) and an EPA-deficient mutant lacking *pfaA* (GenBank: BAJ01172.1) encoding the omega-3 polyunsaturated fatty acid synthase PfaA [28] in the *S. violacea* genome [36], and *Escherichia coli* strain DH5α (TOYOBO Co., Ltd., Osaka, Japan) were used in this study. Hereafter, the EPA-deficient mutant lacking *pfaA* in *S. violacea* was simply designated as the Δ*pfaA* mutant. Marine Broth 2216 (BD Difco, Franklin Lakes, NJ, USA) was used as a medium to culture the *S. violacea* cells, and LB medium (0.5 % Bacto yeast extract, 1 % Bacto tryptone, 1 % NaCl) for *E. coli*

cells. Precipitates arising from autoclaving Marine Broth 2216 were removed by sedimentation for a few days at 4 °C prior to use. Cells were grown in the medium with shaking in 100-ml flasks at 0.1 MPa and 10 °C, or grown as static cultures under pressures of 0.1, 30, 50, and 75 MPa. In the latter case, cells that had been precultured at 0.1 MPa and 10 °C with shaking were diluted in the medium to give an OD_{600} value of 0.01, and the diluted cell suspensions were divided into 15-ml sterilized polypropylene tubes. After sealing with parafilm, the tubes were placed in stainless vessels (PV100-360, Syn Corp., Kyoto, Japan) to apply high hydrostatic pressure. Throughout the study, the temperature was kept at 10 °C, which was slightly higher than the optimal growth temperature of 8 °C for this strain, because of the technical difficulty in cooling the high-pressure optical cell to 8 °C when placed in the fluorescence device (see below).

2.2. Extraction and analysis of fatty acids

Cells of the wild-type strain and the Δ*pfaA* mutant were grown at 0.1 MPa and 10 °C with shaking. The cells were diluted in the medium to give an OD_{600} value of 0.1 and subjected to pressure of 0.1, 30, and 50 MPa for 24 h at 10 °C as described above. After decompression, the cells were immediately collected by centrifugation, washed twice in Tris-Cl buffer (10 mM Tris-Cl, pH 7.5) containing 0.5 M NaCl, and freeze-dried overnight. The freeze-dried cells were extracted in mixtures of methanol/hydrochloride (Wako Pure Chemical Industries, Ltd., Osaka, Japan) to obtain methyl ester-linked fatty acids as described previously [43]. The resulting fatty acid-methyl esters were resolved in hexane and subjected to GC/MS analysis

using a GCMS-QP5050A (Shimadzu Corp., Kyoto, Japan).

2.3. Preparation of POPC vesicles

POPC (Wako Pure Chemical Industries) was dissolved in chloroform, and the solvent was removed by spraying with nitrogen gas. It was suspended in TE buffer (10 mM Tris-Cl, 1 mM EDTA, pH 7.5) at a concentration of 200 μM with a vortex and sonication. The membranes were allowed to swell in TE buffer at 25 °C for 1 h and subsequently labeled with 0.5 μM TMA-DPH at 25 °C for 10 min in the dark.

2.4. Labeling of cells with TMA-DPH

Labeling of *S. violacea* cells with TMA-DPH was carried out essentially as described previously for the yeast *Saccharomyces cerevisiae* [44, 45]. Exponentially growing cells (OD_{600} ~1.0) of the wild-type strain and the Δ*pfaA* mutant at 0.1 MPa and 10 °C were collected by centrifugation at 1,600 × g for 3 min and washed twice with TE buffer containing 0.5 M NaCl. The cells were labeled with 0.5 μM TMA-DPH for 10 min at 10 °C in the dark. After washing twice with the buffer, the labeled cells were placed in a quartz cuvette at 0.1 OD_{600}. Labeling of *E. coli* DH5α cells was carried out at 37 °C in TE buffer without NaCl.

2.5. High-pressure time-resolved fluorescence anisotropy measurement

A high-pressure optical cell with quartz windows capable of applying hydrostatic pressure up to 200 MPa was built (High-pressure optical cell with inner cell, PCI, Syn Corp., Kyoto, Japan). The optical cell was mounted in a FluoroCube (Horiba Ltd., Kyoto, Japan) capable of performing TCSPC with a polarizing device and a 375-nm laser diode operated with a pulse frequency of 1 MHz (NanoLED 375L, Horiba Ltd.). The optical cell and the pressure-generating device are essentially identical to those described previously except that the inner wall of the PCI was coated in black [46]. A bacterial cell sample placed in a quartz cuvette (4 mm × 4 mm) was excited by the laser through one window, and fluorescence was emitted through the other window at 460 nm. Temperature was maintained at 10 °C by circulating cold water in the PCI. Strain birefringence of the quartz windows is caused by increasing hydrostatic pressure, and thereby the polarized lights are depolarized when passing through the windows [47, 48]. We simply calibrated the strain birefringence of the quartz windows for the measurement by determining the maximal anisotropy (r_0) of 1 μM DPH dissolved in mineral oil at each pressure [49].

Fluorescence anisotropy is described by Equation 1, where I_{VV} and I_{VH} are the fluorescence intensities (the two subscripts indicate the orientation of the excitation and emission polarizer, respectively, with H indicating horizontal and V vertical) and $G = I_{HV}/I_{HH}$ is the instrumental factor.

$$r(t) = [I_{VV}(t) - G\, I_{VH}(t)]/[I_{VV}(t) + 2G\, I_{VH}(t)] \qquad (1)$$

The simplest model of the restricted motion of fluorochromes in the membrane, based on the Brownian diffusion of the label in a cone with a wobbling diffusion constant, leads to the following single exponential approximation of the anisotropy decay with time, $r(t)$ [50]:

$$r(t) = (r_0 - r_\infty) \cdot \exp(-t/\theta) + r_\infty \quad (2)$$

where r_∞ stands for limiting anisotropy, and θ (ns) for rotational correlation time. The order parameter (S) is calculated to obtain structural information on the membrane according to the following equation:

$$S = (r_\infty / r_0)^{1/2} \quad (3)$$

The rotational (wobbling) diffusion coefficient (D_w) was calculated to obtain the dynamic nature of the membrane according to the following equation:

$$D_w = (r_0 - r_\infty)/6\theta r_0 \quad (4)$$

An approximation of the fluorescence decay with time, $I(t)$, is described by the following equation containing three exponential discrete decay components:

$$I(t) = A_1 \cdot \exp(-t/\tau_1) + A_2 \cdot \exp(-t/\tau_2) + A_3 \cdot \exp(-t/\tau_3) \quad (5)$$

where τ is the fluorescence lifetime, and A the amplitude of each fraction. For most experiments in this study, the goodness of fit, as expressed by χ^2, was improved by the use of a triexponential rather than biexponential or monoexponential fluorescence decay function. In this study, data are also expressed as mean τ ($<\tau>$) according to the following equation:

$$<\tau> = A_1 \cdot \tau_1 + A_2 \cdot \tau_2 + A_3 \cdot \tau_3 \quad (6)$$

where A is the amplitude of each fraction.

3. Results

3.1. EPA is required for growth in S. violacea under high pressure

The wild-type strain DSS12 grew equally at 0.1, 30, and 50 MPa at 10 °C with almost the same growth rate (approximate doubling time; T_d ~4 h), and exhibited a reduced growth rate at 75 MPa (T_d ~11 h) (Fig. 1). The Δ*pfaA* mutant grew at 0.1 and 30 MPa with a similar growth rate (T_d ~6 h), but exhibited impaired growth at 50 MPa (T_d ~10 h) and 75 MPa (T_d ~24 h). Therefore, EPA is not required for growth at lower pressures of 0.1 and 30 MPa, but becomes indispensable for growth at higher pressures of 50 and 75 MPa. The upper limit of pressure for growth of the Δ*pfaA* mutant was measurably different from that observed in a previous experiment using a large-scale culture (1.5 liters) in the DEEP-BATH system, in which the growth was inhibited at 30 MPa and 8 °C [37]. This could be due to differences in culture scale, temperature, or stirring effect of the medium between the two experimental conditions.

3.2. Construction of a system employing high-pressure time-resolved fluorescence anisotropy measurement

To investigate the effects of high pressure on membrane properties that are characterized by membrane order, acyl chain motion, and hydration, we constructed a system that enabled high-pressure time-resolved fluorescence anisotropy measurement (HP-TRFAM). It comprises a high-pressure optical cell, high-pressure pump, and TCSPC device (FluoroCube) (Fig. 2A and Experimental procedure). First, to correct the strain birefringence of the quartz windows simply, the r_0 values for DPH (1 μM) in mineral oil were determined under various hydrostatic pressures using the fact that the r_0 values for DPH in meneral oil do not change by

applying pressure. The measured r_0 of DPH at 0.1 MPa was 0.348 ± 0.001 (n = 3), which was nearly identical to its theoretical value of 0.36 [38], and was almost unchanged at pressures up to 50 MPa (0.341 ± 0.001, n = 3). However, the birefringence of the window became considerable at pressures greater than 50 MPa, declining to 0.189 ± 0.002 (n = 3) at 200 MPa (Fig. 2B). Therefore, to determine the correct r_0 and r_∞ values at each pressure, we multiplied r_0 and r_∞ that had been measured under high pressure by the correction coefficients, 1.016 (25 MPa), 1.019 (50 MPa), 1.066 (75 MPa), 1.149 (100 MPa), 1.381 (150 MPa), and 1.838 (200 MPa) throughout the analysis.

To evaluate the performance of this system, we first observed the fluid-to-gel transition of a model POPC membrane under varied pressures and temperatures. The main transition (L_β/L_α) temperature (T_m) of POPC is −4.6 °C at 0.1 MPa and 14.6 °C at 100 MPa (dT_m/dP = 0.192 °C•MPa^{-1}) [22], and hence the main transition occurs at 76.1 MPa at 10 °C and at 128.2 MPa at 20 °C. Figure 3A shows a typical example of the corrected anisotropy decay of TMA-DPH in the POPC membrane measured at 0.1 MPa and 100 MPa at 10 °C. Apparently, the rotational motion of TMA-DPH was highly restricted at 100 MPa where the POPC membrane was in the L_β phase with r_∞ of about 0.3. In contrast, r_∞ was about 0.12 at 0.1 MPa where the membrane was in the L_a phase. Figure 3B illustrates the changes in the order parameter S of the POPC membrane at 10 and 20 °C as a function of pressure. S was 0.704 ± 0.004 (n = 3) at 0.1 MPa and 10 °C. S gradually increased up to 50 MPa, followed by a steep increase at around 76.1 MPa at which the membrane experienced the transition from the L_α to L_β phase. At 0.1 MPa and 20 °C, when the membrane was in the L_a phase, S was 0.655 ± 0.016 (n = 3), which was lower than that at 10 °C. S gradually increased up to 100 MPa,

followed by a steep increase at around 128.2 MPa when the membrane experienced the phase transition. The rotational diffusion coefficient D_w characterizes the degree of acyl chain motion corresponding to the occurrence of voids within the lipid bilayer. D_w for TMA-DPH was greater at 20 °C (31.3 μs^{-1} ± 1.6, n = 3) than at 10 °C (18.5 μs^{-1} ± 0.9, n = 3) and decreased with pressure in concert with the gradual increase in S in the L_α phase (Fig. 3B, C). In the L_β phase at pressures above 75 MPa (10 °C) and 100 MPa (20 °C), we failed to perform an exponential approximation of the anisotropy decay with time to determine the rotational correlation time for TMA-DPH motion within the highly ordered POPC gel (Fig. 3C). Our results for pressure-induced fluid-to-gel transition of the POPC membrane are consistent with a previous result obtained at 15 °C [48].

The fluorescence lifetime τ of TMA-DPH depends on the dielectric constant of the membrane interfacial region which results from water penetration, i.e., hydration [51, 52]. At 0.1 MPa, the POPC membrane exhibited a shorter mean fluorescence lifetime $<\tau>$ at 20 °C, 4.20 ± 0.11 ns (n = 3), than that at 10 °C, 4.94 ± 0.04 (n = 3), indicating that the POPC membrane is more hydrated at higher temperature (20 °C) when it is in the L_α phase (Fig. 3D). Upon the fluid-to-gel transition, $<\tau>$ sharply increased at 75 MPa (10 °C) and 125 MPa (20 °C), followed by a linear decrease with pressure (Fig. 3D). This indicates that the POPC membrane is dramatically dehydrated upon the transition from the liquid crystalline to the gel phase. It is worth noting that the degree of hydration is temperature dependent in the L_α phase while it is independent of temperature in the L_β phase (Fig. 3D). The linear decrease in $<\tau>$ at higher pressures ranges (125−200 MPa) was also reported by Bernsdorff et al. and they interpreted this as meaning that TMA-DPH may vertically displace toward the interfacial

region of the POPC membrane at higher pressures with a change in the rotational mode [48].

3.3. EPA deficiency alters dynamic membrane structure under high pressure

With the newly designed system employing HP-TRFAM, we elucidated the membrane property of *S. violacea* cells under high pressure and investigated how the loss of EPA influenced the dynamic structure of the membrane. Cells of the wild-type strain and the Δ*pfaA* mutant were grown at 0.1 MPa and 10 °C and then labeled with 0.5 μM TMA-DPH. The fluorescent dye is nontoxic at this concentration because no measurable change in morphology, motility, and growth was observed in the cells (data not shown). TMA-DPH as well as DPH predominantly localizes to the inner membrane rather than the outer membrane in gram-negative bacteria (J. T. Trevors, personal communication). In addition, treatment of the cells with lysozyme in an isotonic buffer (phosphate buffer containing 0.5 M NaCl) had no measurable effect on the fluorescence intensity, S, D_w, and $\langle\tau\rangle$ in TMA-DPH labeled cells, confirming that TMA-DPH molecules predominantly localize in the inner membrane (data not shown).

We found that the membrane of *S. violacea* wild-type cells was highly ordered at 0.1 MPa, exhibiting the order parameter S of 0.900 ± 0.021 (n = 3) (Table 1). As a comparison, the membrane of *E. coli* strain DH5α, which was grown at 37 °C, showed a lower S of 0.864 ± 0.023 (n = 4) at 37 °C. However, S of the *E. coli* membrane was 0.936 ± 0.025 (n = 4) at 10 °C, which was much higher than that of *S. violacea* at 10 °C. Thus, the lipid composition of *S. violacea* is likely to offset the direct packing effect of low temperature to maintain

optimal membrane fluidity. Increasing pressures of 30−150 MPa did not significantly affect *S* for the wild-type *S. violacea* membrane ($P > 0.2$ as compared with 0.1 MPa) (Table 1, Fig. 4A). This indicates that the membrane containing EPA was rigid and was no longer ordered by applying further hydrostatic pressure. This is seemingly analogous to the characteristic of the gel phase of the POPC membrane where *S* no longer increased at pressures greater than 75 MPa at 10 °C and greater than 125 MPa at 20 °C (Fig. 3B). Preculture of the cells at 30 or 50 MPa for 1−2 days did not significantly affect *S* values (data not shown). Upon the loss of *pfaA*, *S* decreased from 0.9 to 0.878 ± 0.007 at 0.1 MPa ($n = 3$). Interestingly, the Δ*pfaA* membrane became ordered as pressure increased with respect to the increase in *S* (Fig. 4A). We speculate that the loss of EPA creates more spaces within the lipid bilayer, and thereby the Δ*pfaA* membrane would be prone to become compressed by high pressure. Because the membrane is a heterogeneous mixture in terms of lipid composition, there is no cooperative phase transition, unlike the POPC membrane (Fig. 3B). In concert with reduced membrane order, the rotational motion of acyl chains was accelerated in the Δ*pfaA* membrane with respect to the increased rotational diffusion coefficient D_w from 5.4 ± 1.0 μs^{-1} ($n = 3$) to 7.1 ± 0.5 μs^{-1} ($n = 3$) (Table 1 and Fig. 4B). In both strains, D_w decreased with pressure as a possible restriction of acyl chain motion.

3.4. EPA deficiency affects hydration states of the membrane under high pressure

There was a marginal difference in the mean fluorescence lifetime $\langle\tau\rangle$ of TMA-DPH between the wild-type (5.60 ± 0.05 ns, $n = 3$) and the Δ*pfaA* membrane (5.78 ± 0.08, $n = 3$) at

0.1 MPa (Fig. 4C). The $<\tau>$ values in both membranes were closer to that observed in the gel phase of the POPC membrane (5.56 ± 0.03 ns at 100 MPa and 10 °C) rather than to that in the liquid crystalline phase (4.94 ± 0.04 ns at 0.1 MPa and 10 °C), as if the membrane of *S. violacea* were in the gel-like phase. We found that $<\tau>$ linearly decreased with pressure in the wild-type and the Δ*pfaA* membrane in a manner analogous to the POPC membrane in the gel phase (Fig. 4C). To account for this result, we determined the fractional distribution of the fluorescence lifetime of TMA-DPH in the wild-type and Δ*pfaA* membrane to give three lifetime components, τ_1 (long lifetime, LLC), τ_2 (medium lifetime, MLC), and τ_3 (short lifetime, SLC), along with their amplitudes. In the wild-type strain, the LLC (9.03 ± 3.61 ns, 43.2 ± 10.0 %, n = 3) and MLC (3.61 ± 0.44 ns, 47.0 ± 8.13 %, n = 3) occurred at almost the same ratio, suggesting that there are two distinct membrane domains, with differing degrees of hydration (Fig. 5, Table 2). While the two hypothetical membrane domains occurred equally in the wild-type membrane, the more hydrated membrane domain (MLC) constituted measurably a larger portion of the membrane in the Δ*pfaA* mutant (MLC, 4.23 ± 0.47 ns, 54.4 ± 7.7 %, n = 3; LLC, 9.40 ± 0.77 ns, 36.6 ± 8.6 %, n = 3). In our preliminary observation, lipid vesicles reconstituted after the extraction of the membrane with chloroform exhibited a relatively homogenous fluorescence lifetime distribution of TMA-DPH in both strains comprising of 16 ns of LLC, 5 ns of MLC and 1 ns of SLC, along with their amplitudes of 8 %, 84 % and 8 %, respectively. Accordingly, membrane embedded proteins and/or the protein-lipid interactions play a role in maintaining membrane heterogeneity in terms of hydration. With higher pressure, the LLC appeared to decrease while the MLC increased in the wild-type strain, and this trend was more pronounced in the Δ*pfaA* mutant (Fig. 5, Table 2).

In thermodynamic terms, high hydrostatic pressure prefers an equilibrium state with a smaller system volume. Therefore, it is possible that the two domains with varied hydration states exist in dynamic equilibrium in the cell membrane of both strains, and the system volume is smaller in the hydrated state (MLC) than in the dehydrated state (LLC). Consequently, high pressure confers dominancy of the MLC, which is responsible for the decrease in $<\tau>$. Although the biological relevance of varied hydration states of the membrane and whether the two fractions form laterally segregated membrane domains, like lipid rafts in eukaryotic cells [53, 54] are still unclear, EPA partially acts on the membrane to maintain the two fractions in an equal ratio in living cells under high pressure. However, we cannot exclude the possibility that applying high pressure causes the positional change of TMA-DPH in the membrane in addition to affecting the hydration state.

3.5. Loss of EPA results in an increase in the level of palmitoleic acid

To account for the distinct membrane property between the wild-type strain and Δ*pfaA* mutant, we analyzed the fatty acid composition in the wild-type strain and the Δ*pfaA* mutant cells (Fig. 6). The major fatty acids produced by the wild-type strain include (shown as the systematic name followed by the common name) C16:1 (24.4 ± 0.6 %; *cis*-9-hexadecenoic acid, palmitoleic acid), C16:0 (19.5 ± 0.2 %; hexadecanoic acid, palmitic acid), C20:5 (10.5 ± 0.6 %; 5,8,11,14,17-eicosapentaenoic acid, EPA), i-C15:0 (10.1 ± 0.1 %; isopentadecanoic acid, 13-methylmyristic acid), C14:0 (8.6 ± 0.1 %; tetradecanoic acid, myristic acid), 3-OH C14:0 (7.3 ± 0.3 %; 3-hydroxytetradecanoic acid, 3-hydroxymyristic acid), C13:0 (7.3 ±

0.5 %; tridecanoic acid, tridecanoic acid), C12:0 (4.9 ± 0.6 %; dodecanoic acid, lauric acid), and C18:1 (2.2 ± 0.1 %; cis-9-octadecenoic acid, oleic acid). In aerobic culture with shaking at 0.1 MPa and 10 °C, the fatty acid profile was similar to that obtained in batch culture except for slight increases in C16:1 (26.8 ± 0.3 %) and EPA (13.8 ± 0.3 %). The lipid composition was not significantly altered by varied pressure of 30 and 50 MPa during growth, at least under the culture conditions employed (Fig. 6). We found that the loss of EPA resulted in a dramatic increase in C16:1 (49.0 ±1.4 %, 2.0-fold as compared with the wild-type strain) without any marked changes in the levels of other fatty acid species. The result suggests that *S. violacea* cells compensate for the loss of EPA by specifically increasing the proportion of C16:1 in the membrane. As a consequence of incorporating a substantial degree of the monounsaturated double bond, the Δ*pfaA* membrane is likely to become more interspatial and occupy increased amounts of voids within the acyl chains. This view agrees well with the Δ*pfaA* membrane becoming more compressible with increasing pressure (Fig. 4A, B, see Discussion). A recent functional characterization of polyolefin synthesis genes in *Shewanella oneidensis* MR-1 indicated that disruption of the *pfa* gene cluster resulted in the abolishment of both EPA synthesis and production of the C31:9 product hentriacontanonaene [55]. Because the long-chain hydrocarbon might affect the membrane properties, the C31:9 level of the wild-type strain and the Δ*pfaA* mutant in *S. violacea* should be quantified in our future study (see Discussion).

4. Discussion

In this study, we newly designed a system that enabled HP-TRFAM and elucidated the role of EPA in homeostasis of the membrane in the deep-sea piezophile *S. violacea* strain DSS12. To the best of our knowledge, this is the first report to investigate the dynamic membrane structure of a deep-sea microorganism under the high-pressure conditions of its habitat. The present study focusing on the structural role of EPA in the bacterial membrane *in vivo* could lead to a new way of thinking about the roles of PUFAs in cellular membranes of higher biological systems such as the human brain. High-pressure environments are usually coincident with the occurrence of low-temperature environments. This leads to the speculation that the mechanisms for adapting to high pressure are similar to those used to tolerate low temperature. In general, the membranes of psychrotrophs, psychrophiles, and piezophiles contain increased levels of PUFA which are presumably relevant for retaining greater fluidity at low temperature or high pressure [27, 56]. However, from the standpoint of modulating membrane order, it is unclear why these microbes accumulate PUFA rather than MUFA in their membrane because not all double bonds in a fatty acid have an equivalent impact on membrane physical properties. For example, substituting oleic acid (C18:1) for palmitic acid (C16:0) at the *sn*-2 position of dipalmitoyl-PC to form 16:0/18:1-PC reduced the T_m by 50 °C, whereas the incorporation of a second double bond to form 16:0/18:2-PC lowers the T_m by 22 °C. However, the introduction of a third double bond to form 16:0/18:3-PC increases the T_m by 3 °C. In addition, T_m values for 16:0/16:1- and 16:0/22:6-PC do not differ significantly (−12 and −10 °C, respectively) [57]. Therefore, from the perspective of reducing membrane order, MUFAs are more effective than PUFAs, possibly by interfering with the cooperative liquid-to-gel transition.

S. violacea cells have a substantial level of EPA, and the membrane appears to be highly rigid at its nearly optimal growth temperature of 10 °C. Importantly, the wild-type membrane of *S. violacea* is imperturbable over a wide range of hydrostatic pressures with respect to small effects on S and D_w. Our results counter the generally accepted concept that greater fluidity is a membrane characteristic of microorganisms that inhabit cold, high-pressure environments. We suggest that retaining a certain level of membrane physical property under a wide range of environmental conditions is more important than simply making the membrane more fluid. The loss of EPA mandated a compensatory increase in C16:1 from 24 % into 49 % in the cells. Consistent with the above-mentioned phase behavior of the PC membrane incorporating a double bond(s), the Δ*pfaA* membrane showed a lower S and a higher D_w compared with the wild-type membrane. D_w is correlated with the occurrence of voids within the lipid bilayer, and hence with the rotational acyl chain motion [38, 48, 58]. Therefore, C16:1 at a proportion of 49 % of total fatty acids could occupy more spaces within the lipid bilayer of the Δ*pfaA* mutant than combined C16:1 (24 %) and EPA (11 %) in the wild-type strain. According to ^{2}H-NMR and molecular dynamic simulation studies, DHA is relatively shorter or more compact than more saturated chains. For example, DHA chains have an average length of 0.82 nm at 41 °C compared with 1.42 nm for oleic acid [59]. This is consistent with a DHA conformation with pronounced twists of the chain, which diminishes the separation between the two ends. The conformation of EPA is possibly analogous to DHA in the lipid bilayer, although the structure of both PUFAs in bacterial membranes remains to be elucidated.

One of issues remains to be solved is whether *S. violacea* cells produce C31:9

hentriacontanonaene and the *pfaA* mutant lacks both EPA and C31:9 as observed for *S. oneidensis* MR-1. Deletion mutant for the *ole* gene cluster involved in synthesis of C31:9 exhibited a significantly longer lag phase prior to exponential growth upon the shift of cultivation temperature from 30 °C to 4 °C while the growth rate of the mutant was equivalent to that of the wild-type strain [55]. Although the extent to which such a long-chain hydrocarbon partitions to the cellular membrane is still unclear, C31:9 is assumed to locate in the central region of membrane rather than the interfacial region where TMA-DPH reports the membrane properties. The effect of anesthetic drugs such as ethanol, pentobarbital, chloroform, diethylether, phenytoin, cis-vaccenic acid methylester and cis-vaccenoyl alcohol on the membrane fluidity of mouse brain synaptic plasma membranes [60] and that of short-chain alkyl alcohols and benzyl alcohol on the fluidity of bovine blood platelets [61] were investigated by studies on the fluorescence anisotropy of DPH and TMA-DPH. Both reports describe that the membrane perturbants increase the fluidity of the central region of the lipid bilayer but have no effect on the interfacial region of the membranes. In view of this, it is necessary to determine the level of C31:9 contained in the wild-type and the Δ*pfaA* membrane in *S. violacea* and to perform fluorescence anisotropy measurement using DPH in addition to TMA-DPH.

The membrane of both wild-type and Δ*pfaA* strains appeared to be heterogeneous occurring two distinct membrane domains with differing degrees of hydration. With increasing pressure, the amplitude of the more hydrated membrane faction (MLC) was increased. Our result seemingly counters the general occurrences that membranes become dehydrated upon the liquid-to-gel transition in artificial lipid bilayers [48] or become highly

dehydrated gel-like phase in the plasma membrane of tobacco BY-2 cells [62] when high pressure was applied. We assume that membrane proteins and/or the interactions with lipids could determine the degree of hydration in *S. violacea* membrane. It is worthwhile monitoring the level of hydration of the bacterial membrane under high pressure using environment-sensitive probes, Prodan, Laurdan [63] or F2N12S [62].

The remodeling of fatty acid composition upon the loss of EPA has been shown in *P. profundum* SS9 and *S. livingstonensis* Ac10, in which C16:1 and/or C18:1 were slightly increased, but the effect was not as pronounced as in *S. violacea* DSS12. We assume that the role of EPA differs between these three bacterial strains. In *P. profundum*, EPA is not required but MUFAs are prerequisite for its growth under high pressure and low temperature [17]. *S. livingstonensis* is a psychrotroph but exhibits piezosensitivity with impaired growth at 30 MPa. EPA is specifically required for normal cell division in *S. livingstonensis* at low temperature of 4 °C instead of being a requirement for global membrane fluidity. Exogenously added EPA-containing lipid compensates for the filamentation of the Δ*pfaA* mutant of *S. livingstonensis* at 0.1 MPa and 4 °C [30]. The Δ*pfaA* mutant of *S. violacea* exhibits normal growth at 0.1 MPa and 4 °C but displays filamentation at 30 MPa and 8 °C [37]. While *S. livingstonensis* grows over a wide range of temperature from 4 to 25 °C at 0.1 MPa, *S. violacea* is only capable of growth over a narrow range of temperature from 4 to 10 °C at 0.1 to 75 MPa. Therefore, we assume that while EPA is more specifically required for cell division in *S. livingstonensis* under low temperature, it is prerequisite for preventing the membrane from becoming hyperfluid as well as for normal cell division in *S. violacea*.

Although many correlative data support a link between lipid order and membrane protein

functions, there is an equally compelling body of evidence indicating that membrane organization such as the packing arrangement of lipid headgroups, acyl chain length, or bilayer thickness influences protein functions to a greater extent than membrane order. As an example of the former, Na^+/K^+-ATPase is greatly influenced by membrane order in a Chinese hamster ovary cell line, with a linear decrease in the activity as the order parameter increases with the addition of cholesterol to the membrane lipid [64]. Stroke is a consequence of a reduction in cerebral blood flow. The alterations in the platelet membrane physicochemical (decreased fluidity) and functional (reduced Na^+/K^+-ATPase activity) properties increase proportionally with the severity of stroke as measured using the National Institutes of Health Stroke Scale. These modifications and their interactions with certain vascular risk factors may be involved in the pathogenesis of ischemic injury [65]. As an example of the latter, conversely, the activity of the sarcoplasmic reticular Ca^{2+}-ATPase varies little with the degree of unsaturation and hence membrane order, but depends on the chain length of the reconstituting phospholipid, which indicates that an appropriate bilayer thickness rather than membrane order is required for ATPase activity [66]. A comparison of the respiratory terminal oxidase activity in piezophilic and nonpiezophilic *Shewanella* species indicates that the enzyme of *S. violacea* is the most resistant to high pressure among those of nonpiezophiles tested with respect to the oxidation of *N*,*N*,*N*′,*N*′-tetramethyl-*p*-phenyleneamine as an artificial electron donor [67]. High-pressure resistance of the enzyme activity was at almost the same level in both the wild-type strain and the Δ*pfaA* mutant, implying that the intrinsic property of the membrane protein is the determinant of high-pressure resistance but is not affected by altered lipid species. Conversely, the ToxR protein in *P. profundum* SS9 is regulated by the

alterations of physicochemical properties of the membrane [68]. The lack of knowledge describing the functional and physiological role of microbial PUFA synthesis is significant. In light of these unknown issues, other putative roles of PUFAs are discussed in the context of a potential anti-oxidative role [69, 70] and membrane shielding function [71].

Currently, not many membrane proteins have been investigated with respect to the role of EPA and/or membrane fluidity, but it can be readily understood that the membrane properties differentially influence various membrane proteins under high pressure. Although many issues remain to be elucidated, our approach by means of HP-TRFAM would offer a clue to linking the structural aspects of membranes and membrane protein functions in a quantitative manner.

Acknowledgements

We thank Hiroki Baba and Makoto Nagasawa for technical support in constructing the HP-TRFAM system; and Hitoshi Matsuki, Roland Winter and Jack T. Trevors for valuable discussions. This work was supported by grants from the Japan Society for the Promotion of Science (No. 18658039 and No. 22658031 to F. Abe).

References

[1] A.A. Yayanos, Microbiology to 10,500 meters in the deep sea, Annu.Rev.Microbiol. 49 (1995) 777-805.

[2] F. Abe, C. Kato, K. Horikoshi, Pressure-regulated metabolism in microorganisms, Trends Microbiol. 7 (1999) 447-453.

[3] D.H. Bartlett, Pressure effects on in vivo microbial processes, Biochim.Biophys.Acta 1595 (2002) 367-381.

[4] G.N. Somero, Adaptations to high hydrostatic pressure, Annu.Rev.Physiol. 54 (1992) 557-577.

[5] R. Winter, Synchrotron X-ray and neutron small-angle scattering of lyotropic lipid mesophases, model biomembranes and proteins in solution at high pressure, Biochim.Biophys.Acta 1595 (2002) 160-184.

[6] H. de Smedt, R. Borghgraef, F. Ceuterick, K. Heremans, Pressure effects on lipid-protein interactions in (Na^+ + K^+)-ATPase, Biochim.Biophys.Acta 556 (1979) 479-489.

[7] A.R. Cossins, A.G. Macdonald, The adaptation of biological membranes to temperature and pressure: fish from the deep and cold, J.Bioenerg.Biomembr. 21 (1989) 115-135.

[8] D.H. Bartlett, Microbial adaptations to the psychrosphere/piezosphere, J.Mol.Microbiol.Biotechnol. 1 (1999) 93-100.

[9] I.A. Guschina, J.L. Harwood, Mechanisms of temperature adaptation in poikilotherms, FEBS Lett. 580 (2006) 5477-5483.

[10] G. Feller, Life at low temperatures: is disorder the driving force? Extremophiles 11 (2007) 211-216.

[11] S. Shivaji, J.S. Prakash, How do bacteria sense and respond to low temperature? Arch.Microbiol. 192 (2010) 85-95.

[12] J.R. Hazel, Thermal adaptation in biological membranes: is homeoviscous adaptation the

explanation? Annu.Rev.Physiol. 57 (1995) 19-42.

[13] S. Kaneshina, H. Ichimori, T. Hata, H. Matsuki, Barotropic phase transitions of dioleoylphosphatidylcholine and stearoyl-oleoylphosphatidylcholine bilayer membranes, Biochim.Biophys.Acta 1374 (1998) 1-8.

[14] M.K. Behan, A.G. Macdonald, G.R. Jones, A.R. Cossins, Homeoviscous adaptation under pressure: the pressure dependence of membrane order in brain myelin membranes of deep-sea fish, Biochim.Biophys.Acta 1103 (1992) 317-323.

[15] A.R. Cossins, A.G. Macdonald, The adaptation of biological membranes to temperature and pressure: fish from the deep and cold, J.Bioenerg.Biomembr. 21 (1989) 115-135.

[16] C. Kato, L. Li, Y. Nogi, Y. Nakamura, J. Tamaoka, K. Horikoshi, Extremely barophilic bacteria isolated from the Mariana Trench, Challenger Deep, at a depth of 11,000 meters, Appl.Environ.Microbiol. 64 (1998) 1510-1513.

[17] E.E. Allen, D. Facciotti, D.H. Bartlett, Monounsaturated but not polyunsaturated fatty acids are required for growth of the deep-sea bacterium *Photobacterium profundum* SS9 at high pressure and low temperature, Appl.Environ.Microbiol. 65 (1999) 1710-1720.

[18] S.H. Yang, J.H. Lee, J.S. Ryu, C. Kato, S.J. Kim, Shewanella donghaensis sp. nov., a psychrophilic, piezosensitive bacterium producing high levels of polyunsaturated fatty acid, isolated from deep-sea sediments, Int.J.Syst.Evol.Microbiol. 57 (2007) 208-212.

[19] F. Wang, X. Xiao, H.Y. Ou, Y. Gai, F. Wang, Role and regulation of fatty acid biosynthesis in the response of *Shewanella piezotolerans* WP3 to different temperatures and pressures, J.Bacteriol. 191 (2009) 2574-2584.

[20] J.G. Metz, P. Roessler, D. Facciotti, C. Levering, F. Dittrich, M. Lassner, R. Valentine, K.

Lardizabal, F. Domergue, A. Yamada, K. Yazawa, V. Knauf, J. Browse, Production of polyunsaturated fatty acids by polyketide synthases in both prokaryotes and eukaryotes, Science 293 (2001) 290-293.

[21] R.C. Valentine, D.L. Valentine, Omega-3 fatty acids in cellular membranes: a unified concept, Prog.Lipid Res. 43 (2004) 383-402.

[22] K. Tada, M. Goto, N. Tamai, H. Matsuki, S. Kaneshina, Pressure effect on the bilayer phase transition of asymmetric lipids with an unsaturated acyl chain, Ann.N.Y.Acad.Sci. 1189 (2010) 77-85.

[23] K.R. Applegate, J.A. Glomset, Computer-based modeling of the conformation and packing properties of docosahexaenoic acid, J.Lipid Res. 27 (1986) 658-680.

[24] P.C. Calder, Polyunsaturated fatty acids, inflammatory processes and inflammatory bowel diseases, Mol.Nutr.Food Res. 52 (2008) 885-897.

[25] P.M. Kidd, Omega-3 DHA and EPA for cognition, behavior, and mood: clinical findings and structural-functional synergies with cell membrane phospholipids, Altern.Med.Rev. 12 (2007) 207-227.

[26] M. Hashimoto, H.M. Shahdat, S. Yamashita, M. Katakura, Y. Tanabe, H. Fujiwara, S. Gamoh, T. Miyazawa, H. Arai, T. Shimada, O. Shido, Docosahexaenoic acid disrupts in vitro amyloid beta(1-40) fibrillation and concomitantly inhibits amyloid levels in cerebral cortex of Alzheimer's disease model rats, J.Neurochem. 107 (2008) 1634-1646.

[27] Y. Yano, A. Nakayama, K. Yoshida, Distribution of polyunsaturated Fatty acids in bacteria present in intestines of deep-sea fish and shallow-sea poikilothermic animals, Appl.Environ.Microbiol. 63 (1997) 2572-2577.

[28] E.E. Allen, D.H. Bartlett, Structure and regulation of the omega-3 polyunsaturated fatty acid synthase genes from the deep-sea bacterium *Photobacterium profundum* strain SS9, Microbiology 148 (2002) 1903-1913.

[29] J. Fang, O. Chan, C. Kato, T. Sato, T. Peeples, K. Niggemeyer, Phospholipid FA of piezophilic bacteria from the deep sea, Lipids 38 (2003) 885-887.

[30] J. Kawamoto, T. Kurihara, K. Yamamoto, M. Nagayasu, Y. Tani, H. Mihara, M. Hosokawa, T. Baba, S.B. Sato, N. Esaki, Eicosapentaenoic acid plays a beneficial role in membrane organization and cell division of a cold-adapted bacterium, *Shewanella livingstonensis* Ac10, J.Bacteriol. 191 (2009) 632-640.

[31] F. Wang, P. Wang, M. Chen, X. Xiao, Isolation of extremophiles with the detection and retrieval of *Shewanella* strains in deep-sea sediments from the west Pacific, Extremophiles 8 (2004) 165-168.

[32] Y. Nogi, C. Kato, K. Horikoshi, Taxonomic studies of deep-sea barophilic *Shewanella* strains and description of *Shewanella violacea* sp. nov, Arch.Microbiol. 170 (1998) 331-338.

[33] C. Kato, M.H. Qureshi, Pressure response in deep-sea piezophilic bacteria, J.Mol.Microbiol.Biotechnol. 1 (1999) 87-92.

[34] S. Chikuma, R. Kasahara, C. Kato, H. Tamegai, Bacterial adaptation to high pressure: a respiratory system in the deep-sea bacterium *Shewanella violacea* DSS12, FEMS Microbiol.Lett. 267 (2007) 108-112.

[35] C. Murakami, E. Ohmae, S. Tate, K. Gekko, K. Nakasone, C. Kato, Comparative study on dihydrofolate reductases from *Shewanella* species living in deep-sea and ambient

atmospheric-pressure environments, Extremophiles 15 (2011) 165-175.

[36] E. Aono, T. Baba, T. Ara, T. Nishi, T. Nakamichi, E. Inamoto, H. Toyonaga, M. Hasegawa, Y. Takai, Y. Okumura, M. Baba, M. Tomita, C. Kato, T. Oshima, K. Nakasone, H. Mori, Complete genome sequence and comparative analysis of *Shewanella violacea*, a psychrophilic and piezophilic bacterium from deep sea floor sediments, Mol.Biosyst 6 (2010) 1216-1226.

[37] J. Kawamoto, T. Sato, K. Nakasone, C. Kato, H. Mihara, N. Esaki, T. Kurihara, Favourable effects of eicosapentaenoic acid on the late step of the cell division in a piezophilic bacterium, *Shewanella violacea* DSS12, at high-hydrostatic pressures, Environ.Microbiol.(2011).

[38] L.W. Engel, F.G. Prendergast, Values for and significance of order parameters and "cone angles" of fluorophore rotation in lipid bilayers, Biochemistry 20 (1981) 7338-7345.

[39] H. van Langen, G. van Ginkel, D. Shaw, Y.K. Levine, The fidelity of response by 1-[4-(trimethylammonio)phenyl]-6-phenyl-1,3,5-hexatriene in time-resolved fluorescence anisotropy measurements on lipid vesicles. Effects of unsaturation, headgroup and cholesterol on orientational order and reorientational dynamics, Eur.Biophys.J. 17 (1989) 37-48.

[40] B.R. Lentz, Use of fluorescent probes to monitor molecular order and motions within liposome bilayers, Chem.Phys.Lipids 64 (1993) 99-116.

[41] T.J. Denich, L.A. Beaudette, H. Lee, J.T. Trevors, Effect of selected environmental and physico-chemical factors on bacterial cytoplasmic membranes, J.Microbiol.Methods 52 (2003) 149-182.

[42] J.T. Trevors, Fluorescent probes for bacterial cytoplasmic membrane research, J.Biochem.Biophys.Methods 57 (2003) 87-103.

[43] M. Miyazaki, Y. Nogi, R. Usami, K. Horikoshi, *Shewanella surugensis* sp. nov., *Shewanella kaireitica* sp. nov. and *Shewanella abyssi* sp. nov., isolated from deep-sea sediments of Suruga Bay, Japan, Int.J.Syst.Evol.Microbiol. 56 (2006) 1607-1613.

[44] F. Abe, T. Hiraki, Mechanistic role of ergosterol in membrane rigidity and cycloheximide resistance in *Saccharomyces cerevisiae*, Biochim.Biophys.Acta 1788 (2009) 743-752.

[45] F. Abe, K. Usui, T. Hiraki, Fluconazole modulates membrane rigidity, heterogeneity, and water penetration into the plasma membrane in *Saccharomyces cerevisiae*, Biochemistry 48 (2009) 8494-8504.

[46] F. Abe, K. Horikoshi, Analysis of intracellular pH in the yeast *Saccharomyces cerevisiae* under elevated hydrostatic pressure: a study in baro- (piezo-) physiology, Extremophiles 2 (1998) 223-228.

[47] P.L. Chong, A.R. Cossins, G. Weber, A differential polarized phase fluorometric study of the effects of high hydrostatic pressure upon the fluidity of cellular membranes, Biochemistry 22 (1983) 409-415.

[48] C. Bernsdorff, A. Wolf, R. Winter, E. Gratton, Effect of hydrostatic pressure on water penetration and rotational dynamics in phospholipid-cholesterol bilayers, Biophys.J. 72 (1997) 1264-1277.

[49] J.R. Lakowicz, R.B. Thompson, Differential polarized phase fluorometric studies of phospholipid bilayers under high hydrostatic pressure, Biochim.Biophys.Acta 732 (1983) 359-371.

[50] K. Kinosita Jr, S. Kawato, A. Ikegami, A theory of fluorescence polarization decay in membranes, Biophys.J. 20 (1977) 289-305.

[51] C. Ho, S.J. Slater, C.D. Stubbs, Hydration and order in lipid bilayers, Biochemistry 34 (1995) 6188-6195.

[52] B. Cannon, G. Heath, J. Huang, P. Somerharju, J.A. Virtanen, K.H. Cheng, Time-resolved fluorescence and fourier transform infrared spectroscopic investigations of lateral packing defects and superlattice domains in compositionally uniform cholesterol/phosphatidylcholine bilayers, Biophys.J. 84 (2003) 3777-3791.

[53] M. Edidin, The state of lipid rafts: from model membranes to cells, Annu.Rev.Biophys.Biomol.Struct. 32 (2003) 257-283.

[54] D. Lingwood, H.J. Kaiser, I. Levental, K. Simons, Lipid rafts as functional heterogeneity in cell membranes, Biochem.Soc.Trans. 37 (2009) 955-960.

[55] D.J. Sukovich, J.L. Seffernick, J.E. Richman, K.A. Hunt, J.A. Gralnick, L.P. Wackett, Structure, function, and insights into the biosynthesis of a head-to-head hydrocarbon in *Shewanella oneidensis* strain MR-1, Appl.Environ.Microbiol. 76 (2010) 3842-3849.

[56] F. Wang, X. Xiao, H.Y. Ou, Y. Gai, F. Wang, Role and regulation of fatty acid biosynthesis in the response of *Shewanella piezotolerans* WP3 to different temperatures and pressures, J.Bacteriol. 191 (2009) 2574-2584.

[57] K.P. Coolbear, C.B. Berde, K.M. Keough, Gel to liquid-crystalline phase transitions of aqueous dispersions of polyunsaturated mixed-acid phosphatidylcholines, Biochemistry 22 (1983) 1466-1473.

[58] M. Sutter, T. Fiechter, G. Imanidis, Correlation of membrane order and dynamics derived

from time-resolved fluorescence measurements with solute permeability, J.Pharm.Sci. 93 (2004) 2090-2107.

[59] M.X. Fernandes, J.G. de la Torre, Brownian dynamics simulation of rigid particles of arbitrary shape in external fields, Biophys.J. 83 (2002) 3039-3048.

[60] R.A. Harris, P. Bruno, Membrane disordering by anesthetic drugs: relationship to synaptosomal sodium and calcium fluxes, J.Neurochem. 44 (1985) 1274-1281.

[61] S. Kitagawa, H. Hirata, Effects of alcohols on fluorescence anisotropies of diphenylhexatriene and its derivatives in bovine blood platelets: relationships of the depth-dependent change in membrane fluidity by alcohols with their effects on platelet aggregation and adenylate cyclase activity, Biochim.Biophys.Acta 1112 (1992) 14-18.

[62] Y. Roche, A.S. Klymchenko, P. Gerbeau-Pissot, P. Gervais, Y. Mely, F. Simon-Plas, J.M. Perrier-Cornet, Behavior of plant plasma membranes under hydrostatic pressure as monitored by fluorescent environment-sensitive probes, Biochim.Biophys.Acta 1798 (2010) 1601-1607.

[63] M. Kusube, N. Tamai, H. Matsuki, S. Kaneshina, Pressure-induced phase transitions of lipid bilayers observed by fluorescent probes Prodan and Laurdan, Biophys.Chem. 117 (2005) 199-206.

[64] M. Sinensky, F. Pinkerton, E. Sutherland, F.R. Simon, Rate limitation of (Na^+ + K^+)-stimulated adenosinetriphosphatase by membrane acyl chain ordering, Proc.Natl.Acad.Sci.U.S.A. 76 (1979) 4893-4897.

[65] L. Nanetti, A. Vignini, F. Raffaelli, C. Moroni, M. Silvestrini, L. Provinciali, L. Mazzanti, Platelet membrane fluidity and Na^+/K^+ ATPase activity in acute stroke, Brain Res. 1205

(2008) 21-26.

[66] A.P. Starling, J.M. East, A.G. Lee, Effects of phosphatidylcholine fatty acyl chain length on calcium binding and other functions of the (Ca^{2+}-Mg^{2+})-ATPase, Biochemistry 32 (1993) 1593-1600.

[67] H. Tamegai, Y. Ota, M. Haga, H. Fujimori, C. Kato, Y. Nogi, J. Kawamoto, T. Kurihara, Y. Sambongi, Piezotolerance of the respiratory terminal oxidase activity of the piezophilic *Shewanella violacea* DSS12 as compared with non-piezophilic *Shewanella* species, Biosci.Biotechnol.Biochem. 75 (2011) 919-924.

[68] T.J. Welch, D.H. Bartlett, Identification of a regulatory protein required for pressure-responsive gene expression in the deep-sea bacterium *Photobacterium* species strain SS9, Mol.Microbiol. 27 (1998) 977-985.

[69] T. Nishida, N. Morita, Y. Yano, Y. Orikasa, H. Okuyama, The antioxidative function of eicosapentaenoic acid in a marine bacterium, *Shewanella marinintestina* IK-1, FEBS Lett. 581 (2007) 4212-4216.

[70] H. Okuyama, Y. Orikasa, T. Nishida, Significance of antioxidative functions of eicosapentaenoic and docosahexaenoic acids in marine microorganisms, Appl.Environ.Microbiol. 74 (2008) 570-574.

[71] T. Nishida, R. Hori, N. Morita, H. Okuyama, Membrane eicosapentaenoic acid is involved in the hydrophobicity of bacterial cells and affects the entry of hydrophilic and hydrophobic compounds, FEMS Microbiol.Lett. 306 (2010) 91-96.

Figure legends

Fig. 1. Growth profiles of the wild-type strain and Δ*pfaA* mutant under various pressure conditions. Exponentially growing cells were diluted in Marine Broth 2216 at 0.01 OD_{600}, and the cells were cultivated in a high-pressure chamber at 0.1, 30, 50, and 75 MPa at 10 °C. The OD_{600} value was measured after decompression. Typical data from multiple experiments are shown.

Fig. 2. Construction of a system employing HP-TRFAM. (A) A high-pressure optical cell with quartz windows capable of applying hydrostatic pressure was mounted in a FluoroCube designed to perform TCSPC with a polarizing device and a 375-nm laser diode operated with a pulse frequency of 1 MHz. (B) A calibration curve was derived by measuring r_0 values for 1 μM DPH in mineral oil under various hydrostatic pressures to correct the strain birefringence of the quartz windows caused by high pressure. Data represent mean ± SD from three independent experiments. Error bars are shown within the symbols.

Fig. 3. Phase behavior of the POPC membrane analyzed using HP-TRFAM. The POPC membrane was labeled with 0.5 μM TMA-DPH in TE buffer. (A) Typical examples of anisotropy decays of TMA-DPH embedded in the POPC membrane at 10 °C under pressure of 0.1 MPa and 100 MPa, where the membrane is in the L_a (liquid crystalline) and L_β (gel) phase, respectively. (B) Changes in the order parameter S as a function of pressure. (C) Changes in the rotational diffusion coefficient D_w as a function of pressure. Note that exponential approximation to derive D_w could not be carried out above pressure of 75 MPa at 10 °C and 100 MPa at 20 °C, when the membrane is in the gel phase. (D) Changes in the

mean fluorescence lifetime $<\tau>$ as a function of pressure. Data represent mean ± SD from three independent experiments.

Fig. 4. Effects of high pressure on the dynamic structure of the membrane in the wild-type strain and Δ*pfaA* mutant. Exponentially growing cells were labeled with 0.5 μM TMA-DPH in TE buffer containing 0.5 M NaCl. (A) Changes in the order parameter *S* as a function of pressure. (B) Changes in the rotational diffusion coefficient D_w as a function of pressure. (C) Changes in the mean fluorescence lifetime $<\tau>$ as a function of pressure. Data represent mean ± SD from three independent experiments.

Fig. 5. Effects of high pressure on the fluorescence lifetime of TMA-DPH in the wild-type and Δ*pfaA* membrane. Exponentially growing cells were labeled with 0.5 μM TMA-DPH in TE buffer containing 0.5 M NaCl. (A) Changes in fluorescence lifetime τ of TMA-DPH in the membrane as a function of pressure. (B) Changes in the amplitudes of fluorescence-lifetime components of TMA-DPH in the membrane as a function of pressure. Data represent mean ± SD from three independent experiments. LLC, long lifetime component; MLC, medium lifetime component; SLC, short lifetime component

Fig. 6. Fatty acid composition of the wild-type strain and Δ*pfaA* mutant grown under various pressure conditions. Fatty acids were extracted from late exponentially growing cells at 0.1, 30, and 50 MPa at 10 °C and subjected to GC/MS analysis. Data represent mean ± SD from three independent experiments.

Figure

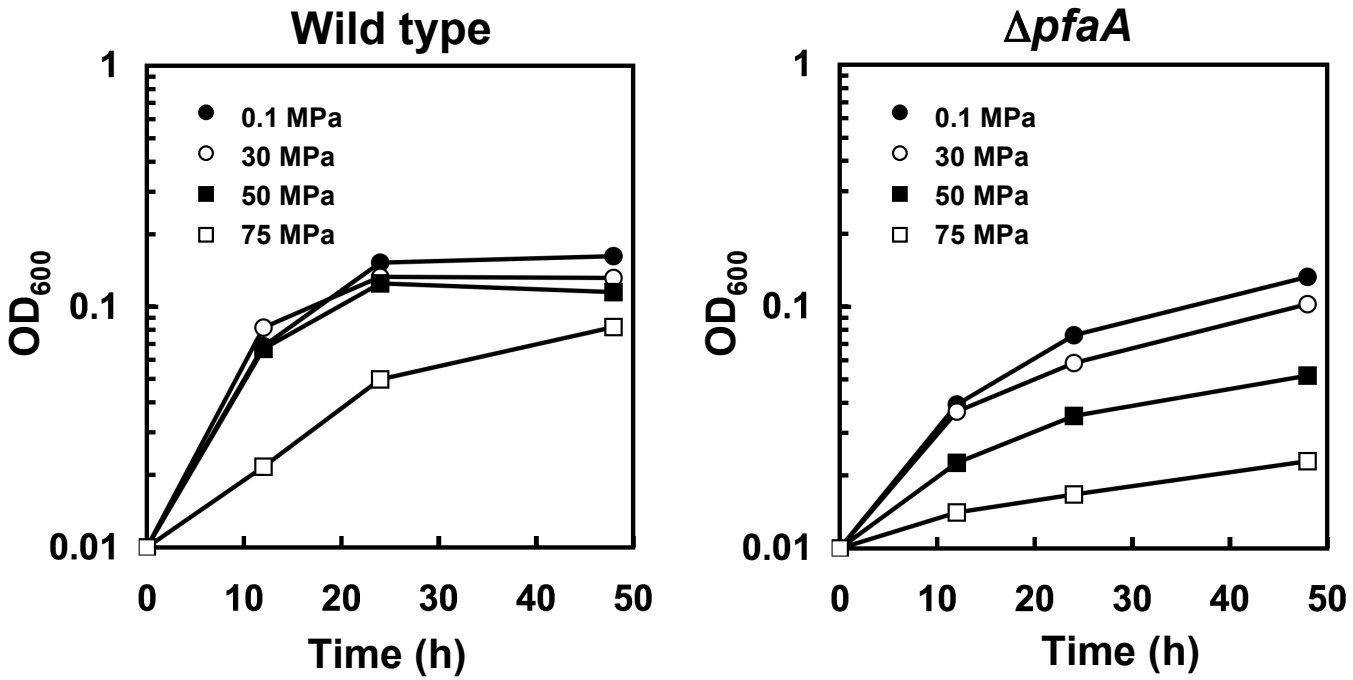

Fig. 1. Usui et al.

Figure

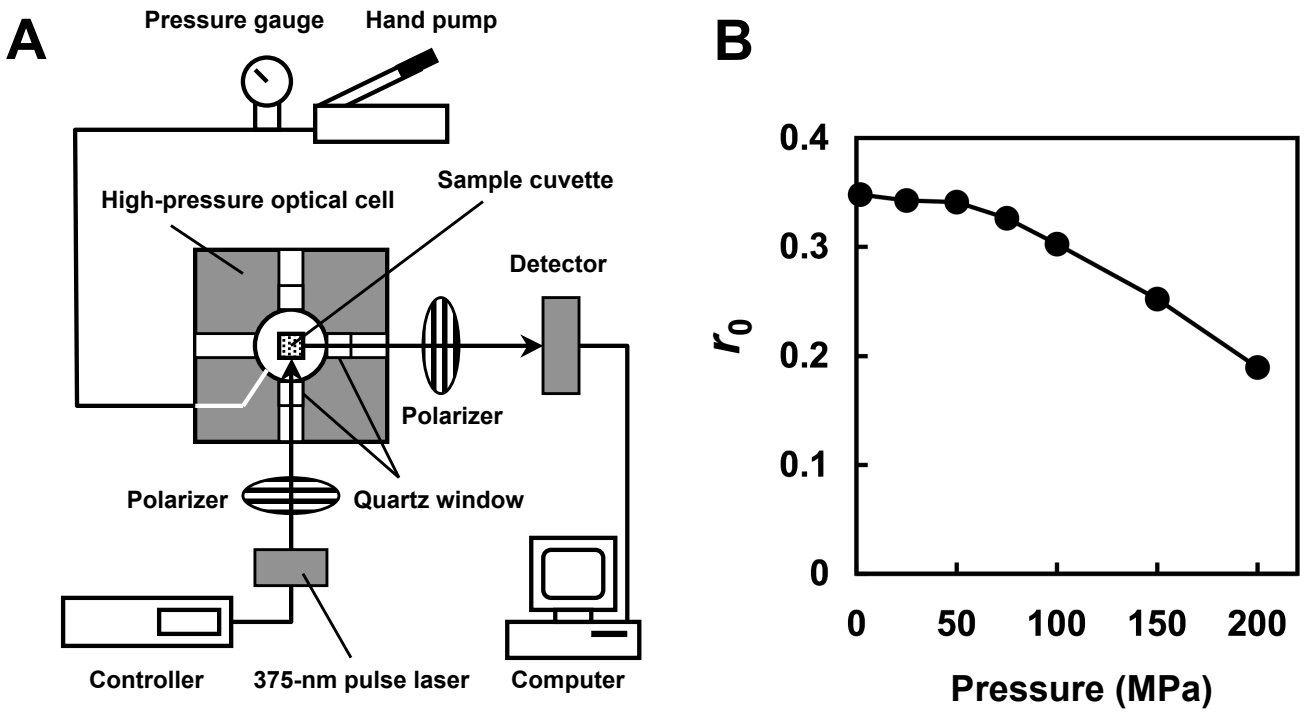

Fig. 2. Usui et al.

Figure

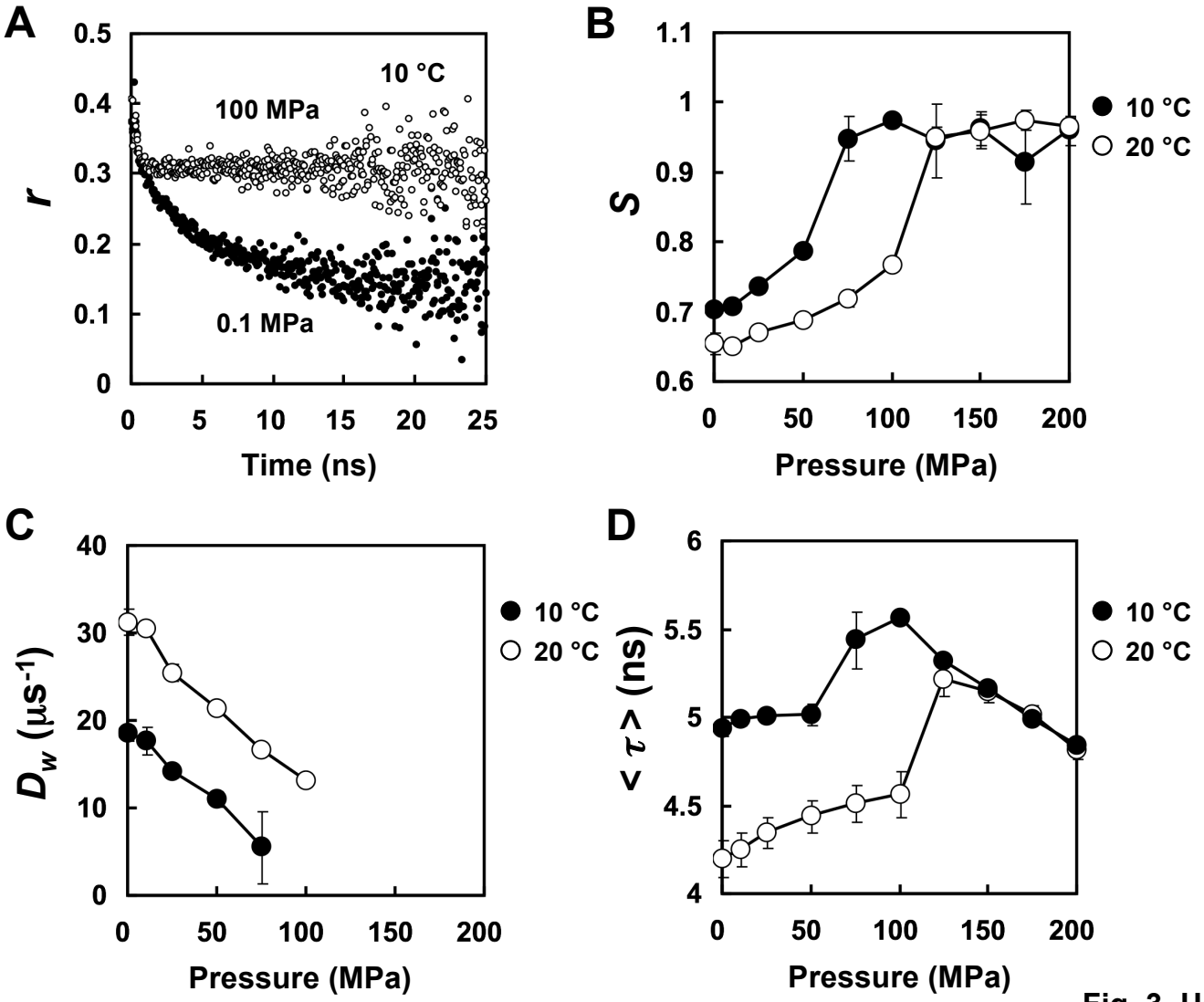

Fig. 3. Usui et al.

Figure

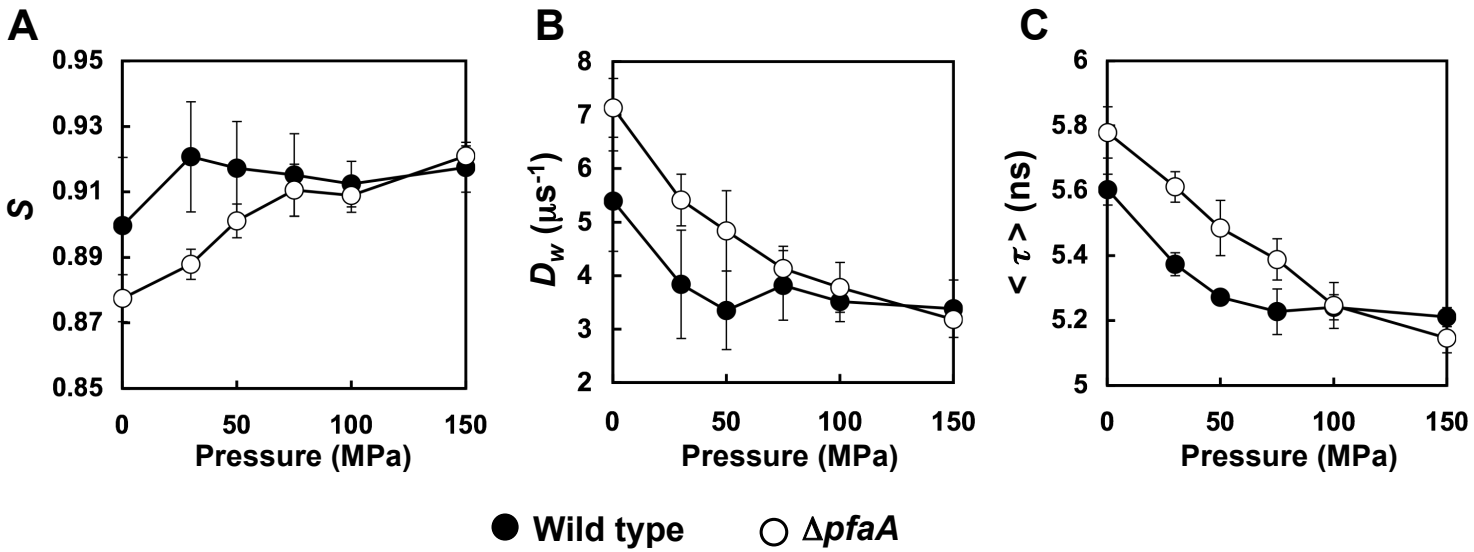

Fig. 4. Usui et al.

Figure

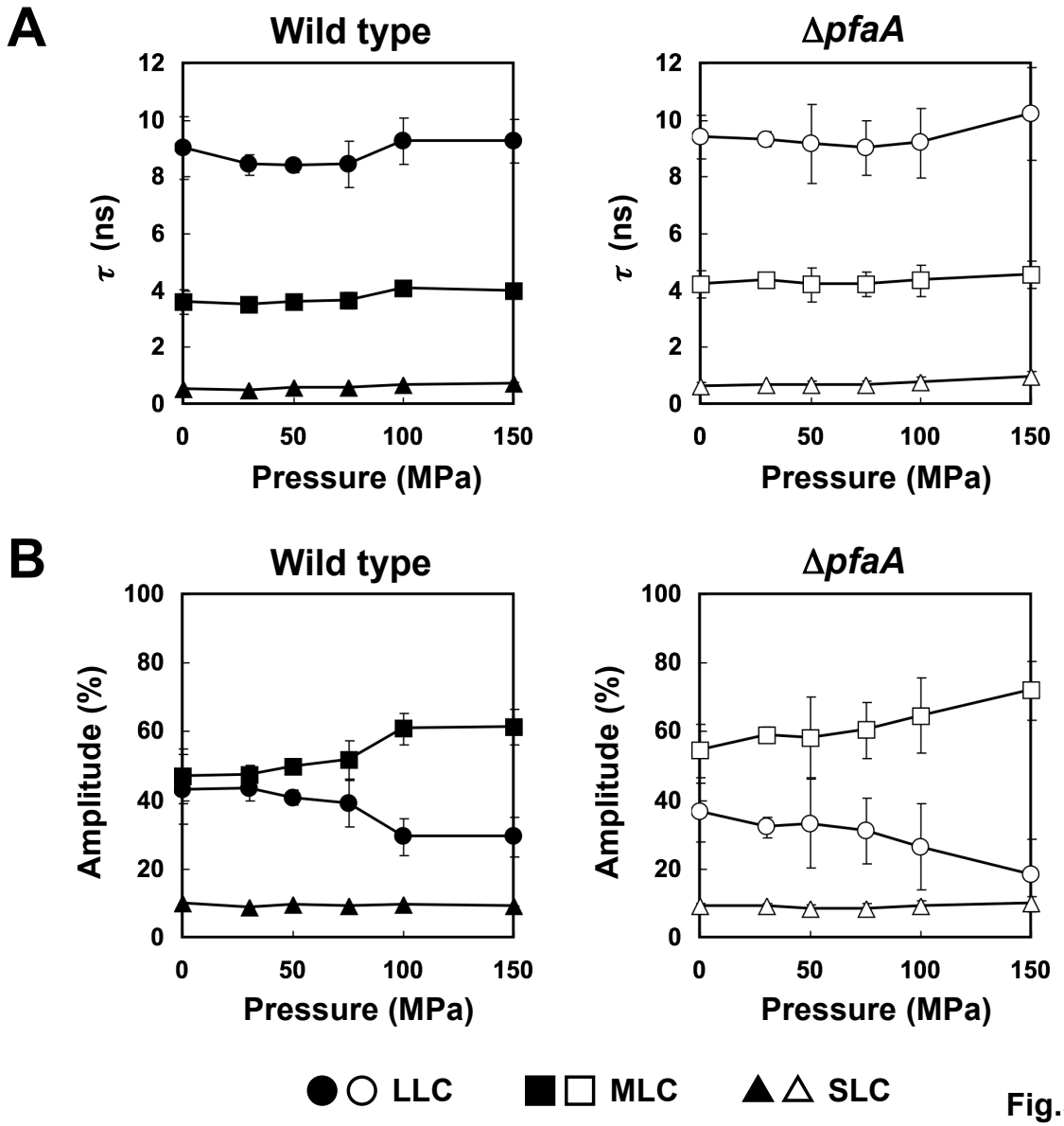

Fig.5. Usui et al.

Figure

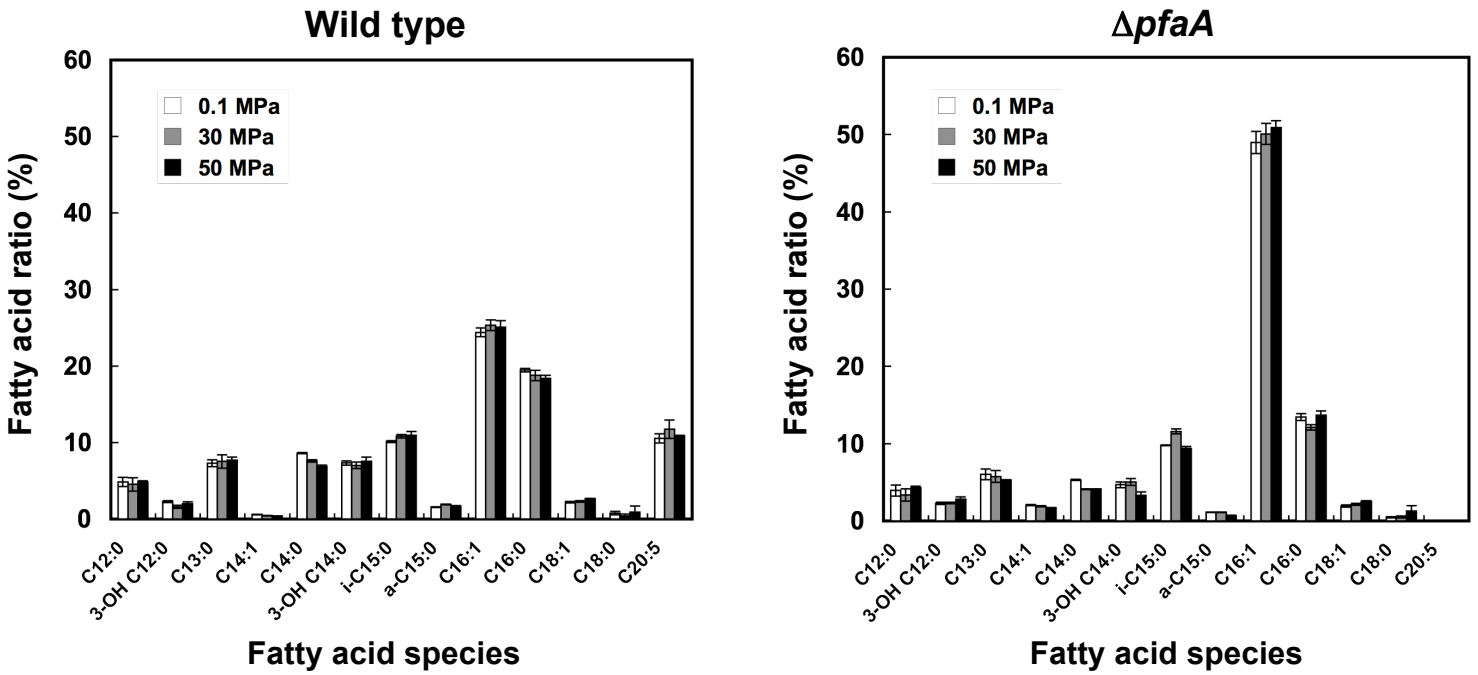

Fig. 6. Usui et al.

Table

Table 1. Effects of hydrostatic pressure on the anisotropy decay of TMA-DPH in the wild-type and Δ*pfaA* cells

	Wild-type cells						
Pressure (MPa)	θ (ns)	r_0	r_∞	S	D_w (μs^{-1})	χ^2	n
0.1	5.9 ± 0.3	0.330 ± 0.008	0.267 ± 0.009	0.900 ± 0.026	5.4 ± 1.1	1.57 ± 0.07	3
30	6.7 ±0.6	0.335 ± 0.006	0.284 ± 0.008	0.921 ± 0.021	3.8 ± 1.2	1.42 ± 0.13	3
50	8.1 ± 1.2	0.332 ± 0.004	0.279 ± 0.009	0.917 ± 0.170	3.3 ± 0.9	1.41 ± 0.10	3
75	7.2 ± 1.6	0.342 ± 0.004	0.287 ± 0.012	0.915 ± 0.015	3.8 ± 0.8	1.35 ± 0.08	3
100	8.0 ± 0.5	0.348 ± 0.007	0.290 ± 0.011	0.912 ± 0.009	3.5 ± 0.5	1.24 ± 0.11	3
150	8.0 ± 1.9	0.367 ± 0.007	0.309 ± 0.012	0.918 ± 0.009	3.4 ± 0.7	1.10 ± 0.01	3
	Δ*pfaA* cells						
Pressure (MPa)	θ (ns)	r_0	r_∞	S	D_w (μs^{-1})	χ^2	n
0.1	5.4 ± 0.4	0.334 ± 0.003	0.257 ± 0.004	0.878 ± 0.009	7.1 ± 0.7	1.37 ± 0.06	3
30	6.6 ± 1.0	0.334 ± 0.001	0.264 ± 0.003	0.888 ± 0.006	5.4 ± 0.6	1.30 ± 0.06	3
50	6.7 ± 1.8	0.330 ± 0.004	0.268 ± 0.006	0.901 ± 0.006	4.8 ± 0.9	1.27 ± 0.08	3
75	7.0 ± 1.6	0.337 ± 0.002	0.279 ± 0.007	0.911 ± 0.010	4.1 ± 0.5	1.22 ± 0.02	3
100	7.8 ± 1.5	0.345 ± 0.005	0.285 ± 0.007	0.909 ± 0.006	3.8 ± 0.6	1.17 ± 0.08	3
150	8.0 ± 0.3	0.364 ± 0.001	0.309 ± 0.002	0.921 ± 0.004	3.2 ± 0.1	1.11 ± 0.00	3

Cells were grown at 0.1 MPa and 10 °C, and analyzed at given hydrostatic pressures.

Measurements were carried out at 10 °C. Data are represented as mean ± SD.

θ, rotational correlation time; r_0, maximum anisotropy; r_∞, limiting anisotropy; S, order parameter;

D_w, rotational diffusion coefficient; n, number of independent experiments.

r_0 and r_∞ have been corrected for strain birefringence of the quartz windows with the correction coefficients, 1.016 (25 MPa), 1.019 (50 MPa), 1.066 (75 MPa), 1.149 (100 MPa) and 1.381 (150 MPa).

Table

Table 2. Effects of hydrostatic pressure on fluorescence lifetime of TMA-DPH in the wild-type and Δ*pfaA* cells

	Wild type								
	LLC		MLC		SLC				
Pressure (MPa)	τ_1 (ns)	A_1 (%)	τ_2 (ns)	A_2 (%)	τ_3 (ns)	A_3 (%)	$<\tau>$	χ^2	*n*
0.1	9.0 ± 1.1	43.2 ± 10.0	3.6 ± 0.4	47.0 ± 8.1	0.5 ± 0.1	9.8 ± 1.9	5.6 ± 0.0	1.51 ± 0.21	3
30	8.4 ± 0.4	43.6 ± 3.6	3.5 ± 0.1	47.5 ± 2.8	0.5 ± 0.0	8.9 ± 0.8	5.4 ± 0.0	1.48 ± 0.14	3
50	8.4 ± 0.2	40.7 ± 2.2	3.6 ± 0.1	49.7 ± 1.8	0.6 ± 0.0	9.6 ± 0.4	5.3 ± 0.0	1.39 ± 0.16	3
75	8.4 ± 0.8	39.2 ± 7.1	3.7 ± 0.3	51.6 ± 5.7	0.6 ± 0.1	9.1 ± 1.4	5.2 ± 0.1	1.35 ± 0.10	3
100	9.3 ± 0.8	29.4 ± 5.4	4.1 ± 0.2	60.9 ± 4.6	0.7 ± 0.1	9.7 ± 0.8	5.2 ± 0.0	1.44 ± 0.12	3
150	9.3 ± 0.8	29.4 ± 5.8	4.0 ± 0.2	61.4 ± 5.1	0.7 ± 0.1	9.2 ± 0.8	5.2 ± 0.0	1.40 ± 0.10	3
	Δ*pfaA*								
	LLC		MLC		SLC				
Pressure (MPa)	τ_1 (ns)	A_1 (%)	τ_2 (ns)	A_2 (%)	τ_3 (ns)	A_3 (%)	$<\tau>$	χ^2	*n*
0.1	9.4 ± 0.8	36.6 ± 8.6	4.2 ± 0.5	54.4 ± 7.7	0.6 ± 0.1	9.0 ± 1.1	5.8 ± 0.1	1.56 ± 0.04	3
30	9.3 ± 0.3	32.1 ± 2.9	4.3 ± 0.1	58.9 ± 2.4	0.7 ± 0.1	9.0 ± 0.8	5.6 ± 0.0	1.48 ± 0.15	3
50	9.2 ± 1.4	33.3 ± 13.0	4.2 ± 0.6	58.2 ± 11.8	0.7 ± 0.1	8.5 ± 1.2	5.5 ± 0.1	1.48 ± 0.06	3
75	9.0 ± 1.0	31.2 ± 9.6	4.2 ± 0.4	60.5 ± 8.1	0.7 ± 0.1	8.4 ± 1.5	5.4 ± 0.1	1.41 ± 0.03	3
100	9.2 ± 1.2	26.3 ± 12.6	4.4 ± 0.5	64.7 ± 10.9	0.8 ± 0.2	9.0 ± 1.7	5.2 ± 0.1	1.39 ± 0.08	3
150	10.2 ± 1.6	18.2 ± 10.6	4.6 ± 0.5	72.0 ± 8.5	1.0 ± 0.2	9.8 ± 2.3	5.1 ± 0.0	1.35 ± 0.09	3

Cells were grown at 0.1 MPa and 10 °C, and analyzed at given hydrostatic pressures.

Measurements were carried out at 10 °C. Data are represented as mean ± SD.

LLC, long lifetime component; MLC, medium lifetime component; SLC, short lifetime component;

τ, fluorescence lifetime; A, amplitude of each fraction; *n*, number of independent experiments.